

Extraction of the S -wave and P -wave DD^* scattering phase shifts using twisted boundary conditions

Masato Nagatsuka^{a,*} and Shoichi Sasaki^a

^aDepartment of Physics, Tohoku University,
Sendai 980-8578, Japan

E-mail: masato.nagatsuka.r4@dc.tohoku.ac.jp,
ssasaki@nucl.phys.tohoku.ac.jp

We present results of a lattice study of the S -wave and P -wave DD^* scattering phase shifts using Lüscher's method under the twisted boundary conditions to investigate the doubly charmed tetraquark T_{cc}^+ observed by the LHCb collaboration. Although the scattering phase shift at zero momentum gives information about the number of bound states according to Levinson's theorem, Lüscher's method under the periodic boundary condition only accesses the scattering phase shifts at some discrete momenta and is not suitable for watching the signal of bound state formation. On the other hand, the twisted boundary condition has the advantage that the scattering phase shift at any momentum can be calculated and that not only the S -wave scattering phase shift but also the P -wave scattering phase shift can be obtained simultaneously. In this study, we perform the simulation for the DD^* and BB^* systems in the $I = 0$ channel using 2+1 flavor PACS-CS gauge ensembles simulated at $m_\pi = 295$ and 411 MeV.

The 41st International Symposium on Lattice Field Theory (LATTICE2024)
28 July - 3 August 2024
Liverpool, UK

*Speaker

1. Introduction

The LHCb collaboration observed a new resonance interpreted to be the doubly charmed tetraquark state T_{cc}^+ in 2021 [1, 2]. It is considered to have isospin $I = 0$ and quark content $cc\bar{u}\bar{d}$ by the experiment. In addition to the discovery, some model calculations indicate that doubly-heavy tetraquark system such as $QQ\bar{u}\bar{d}$ has a bound state if the mass of quark Q is sufficiently heavy, comparable to that of the bottom quark [3, 4].

In order to theoretically confirm the signal of the doubly charmed tetraquark, we calculate the scattering phase shift between D and D^* mesons with lattice QCD using Lüscher's method under twisted boundary conditions [5, 6]. There are several calculation of the scattering phase shift using Lüscher's method [7–9] and using the HAL QCD method [10]. Although these authors aim to find the S -matrix pole located below the DD^* threshold from the DD^* scattering phase shift, the situation is complicated by the fact that the left-hand cut of $DD\pi$ just below the DD^* threshold could give rise to the singularity to the DD^* scattering amplitude [11]. We therefore do not aim to determine the pole condition, rather focus on the detailed information on the scattering phase shift just above the DD^* threshold in this study.

In general, Levinson's theorem tells us that the number of bound states n and the l -wave scattering phase shift at zero momentum $\delta_l(0)$ are related as $\delta_l(0) = n\pi$. Therefore, we can predict the number of bound states in the system by tracing the behavior of scattering phase shift around zero momentum [12]. However, Lüscher's method under the periodic boundary condition only gives the scattering phase shift at a few discrete momenta because the momentum of the center of mass \mathbf{P} is discretized as $(\frac{L\mathbf{P}}{2\pi}) = 0, 1, 2, \dots$ due to the finiteness of the volume.

In this context, twisted boundary conditions plays an important role. We impose the following boundary condition to the wave function $\Psi(\mathbf{x})$ as

$$\Psi(\mathbf{x} + L\mathbf{e}_k) = e^{i\theta_k}\Psi(\mathbf{x}), \quad (1)$$

where \mathbf{e}_k are unit vectors in the direction of the k axis ($k = x, y, z$) and θ_k are real valued twisted angles. Under the twisted boundary condition, the momentum of a plane wave \mathbf{p} are discretized as

$$\mathbf{p} = \frac{2\pi\mathbf{n}}{L} + \boldsymbol{\theta}, \quad \mathbf{n} \in \mathbb{Z}^3 \quad (2)$$

with a twist angle vector $\boldsymbol{\theta} = (\theta_x, \theta_y, \theta_z)$ for the free case. By adjusting the arbitrary parameter θ_k , we can change the ground state energy of two-hadron scattering system, but this requires modifications to the original Lüscher's method as explained in Sec. 2. We can make use of this formula to calculate both S -wave and P -wave scattering phase shifts at low energies in detail.

We therefore perform the calculation of scattering phase shift for the both DD^* and BB^* systems using Lüscher's method under twisted boundary conditions to explore the behavior of the low-energy scattering near the DD^* and BB^* threshold.

Twist angle	$(0, 0, \theta)$	$(\theta, \theta, 0)$	(θ, θ, θ)
Symmetry	C_{4v}	C_{2v}	C_{3v}
label	[001]	[110]	[111]
$\mathcal{M}_{SS}^\theta(q)$	w_{00}	w_{00}	w_{00}
$\mathcal{M}_{SP}^\theta(q)$	$i\sqrt{3}w_{10}$	$i\sqrt{6}w_{11}$	$i3w_{10}$
$\mathcal{M}_{PP}^\theta(q)$	$w_{00} + 2w_{20}$	$w_{00} - w_{20} - i\sqrt{6}w_{22}$	$w_{00} - i2\sqrt{6}w_{22}$

Table 1: Definitions of $\mathcal{M}_{SS}^\theta(q)$, $\mathcal{M}_{SP}^\theta(q)$ and $\mathcal{M}_{PP}^\theta(q)$ for each twist angle ($0 < |\theta| < \pi$).

2. Formulation

2.1 Lüscher's finite size formula and the calculation strategy

For the case of S -wave ($l = 0$) scattering phase shift $\delta_0(k)$, it is possible to be calculated from energy spectra using Lüscher's formula under the periodic boundary condition

$$\cot \delta_0(k) = \frac{1}{\pi^{3/2}q} Z_{00}(1; q^2), \quad q = \frac{Lk}{2\pi}, \quad (3)$$

where the higher partial-wave ($l \geq 4$) contributions are ignored. Since Lüscher proposed the equation, we have seen many different kinds of extensions. Eventually, if the twisted boundary conditions are employed and the higher partial-wave ($l \geq 2$) contributions are ignored, the formula can be summarized as

$$\begin{vmatrix} \cot \delta_0(k) - \mathcal{M}_{SS}^\theta(q) & \mathcal{M}_{SP}^\theta(q) \\ \mathcal{M}_{SP}^\theta(q)^* & \cot \delta_1(k) - \mathcal{M}_{PP}^\theta(q) \end{vmatrix} = 0, \quad (4)$$

where $\mathcal{M}_{SS}^\theta(q)$, $\mathcal{M}_{SP}^\theta(q)$ and $\mathcal{M}_{PP}^\theta(q)$ depend on the direction of θ , as shown in Table 1 [6]. w_{lm} that appears in the table are defined as

$$w_{lm} = \frac{1}{\pi^{3/2}\sqrt{2l+1}q^{l+1}} Z_{lm}^\theta(1; q^2)^*. \quad (5)$$

The generalized zeta function is also defined as

$$Z_{lm}^\theta(1; q^2) = \sum_{\mathbf{r} \in \Gamma_\theta} \frac{\mathcal{Y}_{lm}(\mathbf{r})}{(\mathbf{r}^2 - q^2)}, \quad (6)$$

where $\Gamma_\theta = \{\mathbf{r} | \mathbf{r} = \mathbf{n} + \frac{\theta}{2\pi}, \mathbf{n} \in \mathbb{Z}^3\}$ and $\mathcal{Y}_{lm}(\mathbf{r}) = |\mathbf{r}|^l Y_{lm}(\mathbf{r})$.

This formula claims that the angular momentum states can be highly mixed each other and it is not reasonable to truncate the effect of P -wave ($l = 1$) scattering for $0 < |\theta_k| < \pi$. In our research, we make use of the property to extract not only the S -wave scattering phase shift, but also the P -wave scattering phase shift according to the following strategy divided into three steps [6].

1. Calculate the S -wave scattering phase shifts using Eq. (3) for special angles $\theta = (0, 0, 0)$, $(0, 0, \pi)$, $(\pi, \pi, 0)$ and (π, π, π) . Then, we interpolate the data using the effective range expansion

$$k \cot \delta_0(k) = \frac{1}{a_0} + \frac{1}{2}r_0k^2 + v_0k^4. \quad (7)$$

This treatment is valid near the threshold, where the higher partial-wave ($l \geq 2$) contributions are safely ignored. Indeed, there are no mixing between S -wave and P -wave states for these special angles since the corresponding point group maintains a center of inversion symmetry.

2. Calculate the P -wave scattering phase shift according to Eq. (4) for $\boldsymbol{\theta} = (\theta, \theta, \theta)$ expressed as

$$\cot \delta_1(k) = w_{00}(q) + 2\sqrt{6}\text{Im}\{w_{22}(q)\} + \frac{9w_{10}^2(q)}{\cot \delta_0(k) - w_{00}(q)}. \quad (8)$$

We use the interpolated data sets of $\cot \delta_0$ given by Eq. (7) as inputs in the right hand side of Eq. (8). We also interpolate the obtained P -wave scattering phase shift according to the effective range expansion up to $\mathcal{O}(k^2)$.

3. Finally calculate the S -wave scattering phase shift near the threshold using Eq. (4) for $\boldsymbol{\theta} = (0, 0, \theta)$ expressed as

$$\cot \delta_0(k) = w_{00}(q) + \frac{3w_{10}^2(q)}{\cot \delta_1(k) - w_{00} - 2w_{22}(q)} \quad (9)$$

with help of the interpolated data sets of $\cot \delta_1$ obtained from the second step.

There are two advantages in this strategy. First, S -wave scattering phase shifts near the threshold can be obtained with high resolution. Second, it is also possible to simultaneously obtain the P -wave scattering phase shift only by calculating the irreducible representation (irrep) A_1 of two-hadron states.

2.2 Calculation under the twisted boundary condition

In our simulation we use the twisted boundary condition for the charm and bottom quarks while the periodic boundary condition is used for light quarks. We calculate the charm and bottom quark propagators under the twisted boundary conditions as follows.

Suppose quark fields $q_\theta(\mathbf{x}, t)$ satisfy the twisted boundary condition

$$q_\theta(\mathbf{x} + L\mathbf{e}_j, t) = e^{i\theta_j} q_\theta(\mathbf{x}, t). \quad (10)$$

We can introduce new fields

$$q'(\mathbf{x}, t) = e^{-i\boldsymbol{\theta} \cdot \mathbf{x}/L} q_\theta(\mathbf{x}, t), \quad (11)$$

which obey to the periodic boundary condition. Therefore, for the Wilson-type fermions, we can calculate quark propagators subject to the twisted boundary condition with a simple modification $U_{x,\mu} \rightarrow e^{i\theta_\mu a/L} U_{x,\mu}$ to gauge configurations $U_{x,\mu}$ where $\theta_\mu = (\boldsymbol{\theta}, 0)$ and the lattice spacing a .

In our calculations, we use wall-source operators so that the two-hadron interpolating operators are automatically projected to the trivial irreducible representations of the point group. The wall source operator for $q'(\mathbf{x}, t)$ can be rewritten in terms of $q_\theta(\mathbf{x}, t)$ as

$$q(\mathbf{p}, t) = \sum_{\mathbf{x}} q'(\mathbf{x}, t) = \sum_{\mathbf{x}} q_\theta(\mathbf{x}, t) e^{i\boldsymbol{\theta} \cdot \mathbf{x}/L}, \quad (12)$$

where $\mathbf{p} = \boldsymbol{\theta}/L$. Thus, the wall-source quark operator with twisted angle $\boldsymbol{\theta}$ can be considered as the momentum \mathbf{p} projected operator. We then use wall-source operators to construct the hadron (h) interpolating operator at the source as

$$O_h^{W,k}(\mathbf{p}, t_{\text{src}}) = \sum_{\mathbf{x}} \bar{q}_f(\mathbf{x}, t_{\text{src}}) \Gamma_k \sum_{\mathbf{y}} q_{f'}(\mathbf{y}, t_{\text{src}}) \quad (13)$$

with $\mathbf{p} = (\boldsymbol{\theta}_f - \boldsymbol{\theta}_{f'})/L$, while we use local operators to construct the hadron (h) interpolating operator at the sink

$$O_h^{L,k}(\mathbf{x}, t_{\text{snk}}) = \bar{q}_f(\mathbf{x}, t_{\text{snk}}) \Gamma_k q_{f'}(\mathbf{x}, t_{\text{snk}}), \quad (14)$$

where f and f' denote flavor indices and Γ_k is a gamma matrix. $\Gamma_k = \gamma_k$ ($k = 1, 2, 3$) is chosen for spin-1 mesons, and $\Gamma_k = \gamma_5$ ($k = 5$) is chosen for spin-0 mesons. The index k is omitted hereafter. In case of $h = D$ and D^* (B and B^*) mesons, the twist angles of up and down quarks are fixed to be $\boldsymbol{\theta}_f = \mathbf{0}$, while the twist angle of charm (bottom) quarks is varied so that the momentum \mathbf{p} is finite.

In this study, we only consider the center-of-mass of the two-hadron system. For the two-hadron (DD^*) interpolating operator at the source, we use wall operators given as

$$Q_{DD^*}^W(\mathbf{P} = \mathbf{0}, \mathbf{p}, t_{\text{src}}) = O_D^W(\mathbf{p}, t_{\text{src}}) O_{D^*}^W(-\mathbf{p}, t_{\text{src}}), \quad (15)$$

where the D and D^* operators carry the opposite momentum so as to make zero total momentum of the DD^* system ($\mathbf{P} = \mathbf{0}$). Non-zero \mathbf{p} is responsible for non-zero relative momentum between the D and D^* mesons. For the sink operator, we use a simple product of two local operators and take summation over the spatial sites independently for each operator as

$$Q_{DD^*}^L(\mathbf{P} = \mathbf{0}, t_{\text{snk}}) = \sum_{\mathbf{x}} O_D^L(\mathbf{x}, t_{\text{snk}}) \sum_{\mathbf{y}} O_{D^*}^L(\mathbf{y}, t_{\text{snk}}), \quad (16)$$

where the total momentum of the DD^* system is projected onto zero momentum, when the twist angles of the charm quarks involved in D and D^* mesons are taken in opposite directions with the same angle size.

The usage of the wall-source operators indicates that the resulting two-hadron correlators are already projected to the trivial irrep A_1 of any point group as discussed in Ref. [6]. In addition, for the case of the DD^* or BB^* scattering, since there is only a single spin state, no spin projection is required. For the isospin I of the DD^* or BB^* systems, we focus only on the $I = 0$ channel in this talk.

3. Numerical Results

3.1 Simulation Details

We apply Lüscher's method to explore the DD^* and BB^* scatterings at low energies. For this purpose we perform lattice QCD simulations on a lattice $L^3 \times T = 32^3 \times 64$ with 2+1 flavor PACS-CS gauge configurations, where the simulated pion masses are $m_\pi = 295$ and 411 MeV. Simulation parameters of PACS-CS gauge configurations are summarized in Table 2.

We use nonperturbatively improved clover fermions for up and down quarks while relativistic heavy quark (RHQ) action is used for charm and bottom quarks. Parameters of clover fermions and the RHQ action used in this work are listed in Table 3. The RHQ parameters defined in a Tsukuba-type action [14, 15] have been properly determined in Ref. [16].

β	a (fm)	$L^3 \times T$	$\sim La$ (fm)	c_{SW}
1.9	0.0907(13)	$32^3 \times 64$	2.9	1.715

Table 2: Simulation parameters of 2 + 1 flavor PACS-CS gauge configurations, generated using the Iwasaki gauge action and Wilson clover fermions [13].

3.2 Analysis of scattering phase shifts

Making use of the operators defined in Sec. 2, we calculate masses of D , D^* , B and B^* mesons and energies of the DD^* and BB^* systems. The masses of each mesons are tabulated in Table. 5. We are also able to calculate the scattering momentum k from the total energy of two-meson system by using the relation

$$W = \sqrt{k^2 + M_h^2} + \sqrt{k^2 + M_{h^*}^2} \quad (h = D, B). \quad (17)$$

After we obtain k^2 for each twisted angle, we can use Lüscher's method to calculate the S -wave scattering phase shift $\delta_0(k)$ and P -wave scattering phase shift $\delta_1(k)$ according to the three steps described in Sec. 2.

First, we calculate S -wave scattering phase shift $\delta_0(k)$ for specific four angles $\boldsymbol{\theta} = (0, 0, 0)$, $(0, 0, \pi)$, $(\pi, \pi, 0)$ and (π, π, π) where we can use Eq. (3). As a typical example, we show the $k \cot \delta_0$ as a function of q^2 for the case of the $I = 0$ DD^* scattering with $m_\pi = 411$ MeV in the left panel of Fig 1. We observe that $k \cot \delta_0$ is monotonically increasing within this range and we interpolate the four data points expressed as circles. Next, we calculate P -wave scattering phase shift $\delta_1(k)$ from data sets of $\boldsymbol{\theta} = (\theta, \theta, \theta)$ using Lüscher's formula (8) with a help of information obtained beforehand on S -wave. We observe the behavior of $k^3 \cot \delta_1$ as a function of q^2 in the right panel of Fig. 1. We fit these data as the linear function of q^2 . We then can calculate the S -wave scattering phase shifts near the threshold from data sets of $\boldsymbol{\theta} = (0, 0, \theta)$ using Lüscher's formula (9) with a help of the P -wave information obtained from the data sets of $\boldsymbol{\theta} = (\theta, \theta, \theta)$. As shown in the left panel of Fig 1, the results of S -wave $k \cot \delta_0(k)$ obtained near the threshold (diamond symbols) fill a gap between two data points obtained from $\boldsymbol{\theta} = (0, 0, 0)$ and $(0, 0, \pi)$.

The above procedure was carried out for four different combinations of two light quarks ($m_\pi = 295$ and 411 MeV) and two heavy-flavor quarks (charm and bottom). The results for δ_0 and δ_1 are shown as a function of the two-meson energy E measured from the respective thresholds in Fig. 2 and Fig 3.

Both S -wave (Fig. 2) and P -wave (Fig 3) scattering phase shifts are positive, reflecting the attractive interaction between the D and D^* (B and B^*) states in the $I = 0$ channel. Although neither T_{cc} nor T_{bb} states could be observed as deeply bound states of DD^* or BB^* in our study, the weak attraction seen in both channels becomes stronger as m_π decreases from 411 MeV to 295 MeV. Especially, for the BB^* case, the unitary limit ($\lim_{k \rightarrow 0} k \cot \delta_0(k) \approx 0$) is reached at $m_\pi = 295$ MeV, and the peculiar behavior of the scattering phase shift at $E = 0$ MeV suggests the formation of a shallow bound state ¹. We can therefore expect a deeply bound state at lighter pion masses.

¹The isospin projection was incorrect in our previous analysis where there was no sign of bound state formation.

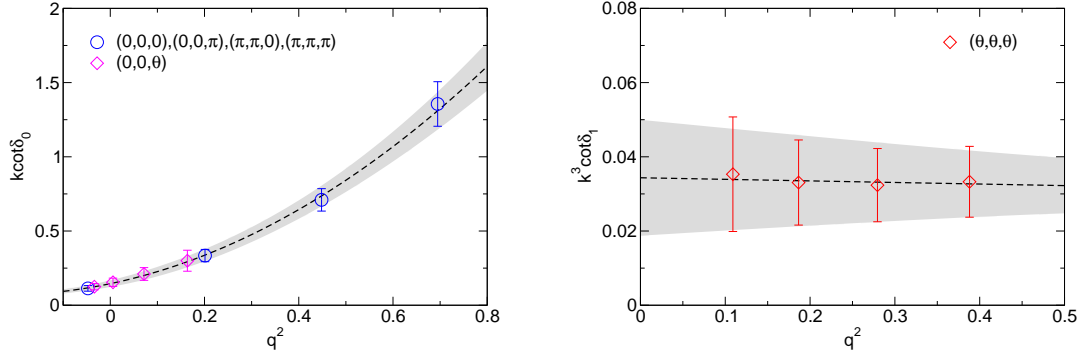


Figure 1: Left: $k \cot \delta_0$ as a function of q^2 for the case of the $I = 0$ DD^* scattering at $m_\pi = 411$ MeV. Right: $k^3 \cot \delta_1$ as a function of q^2 for the case of the $I = 0$ DD^* scattering at $m_\pi = 411$ MeV.

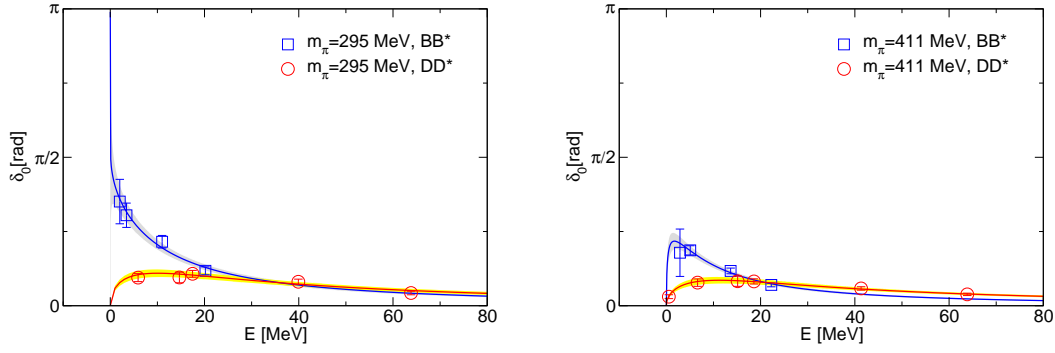


Figure 2: S -wave scattering phase shifts for the DD^* and BB^* scatterings in the $I = 0$ channel: $m_\pi = 295$ MeV (left) and $m_\pi = 411$ MeV (right).

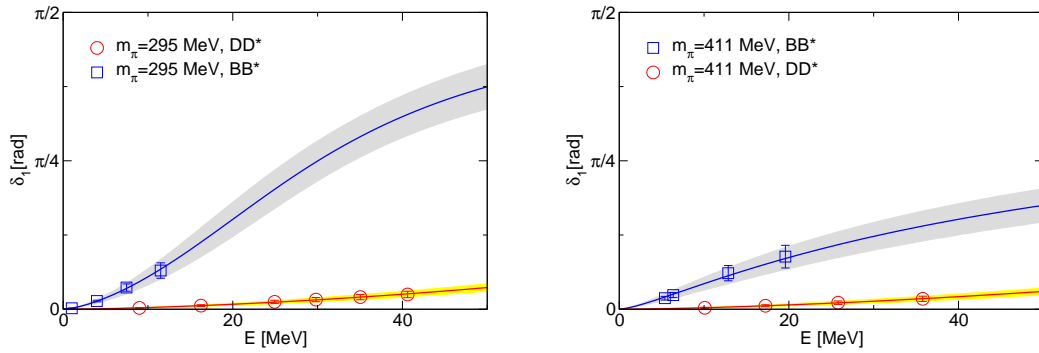


Figure 3: P -wave scattering phase shifts for the DD^* and BB^* scatterings in the $I = 0$ channel: $m_\pi = 295$ MeV (left) and $m_\pi = 411$ MeV (right).

Flavor	κ_h	ν	r_s	c_B	c_E
Charm	0.10819	1.2153	1.2131	2.0268	1.7911
Bottom	0.03989	2.9570	2.5807	4.0559	2.8357

Table 3: Parameters of the RHQ action for charm and bottom quarks used in this work. The parameter set of the charm quark was determined in Ref. [16].

Ensemble	(κ_{ud}, κ_s)	M_π [MeV]	# of configs.
A	(0.13770, 0.13640)	295(2)	799
B	(0.13754, 0.13640)	411(1)	450

Table 4: Simulation parameters of PACS-CS configurations [13].

Ensemble	M_D [GeV]	M_{D^*} [GeV]	M_B [GeV]	M_{B^*} [GeV]
A	1.877(2)	2.030(4)	5.258(3)	5.310(4)
B	1.901(2)	2.056(4)	5.291(5)	5.344(7)

Table 5: Mass spectrum of D , D^* , B and B^* mesons.

4. Summary

In this talk, we presented our results on the calculation of the S -wave and P -wave scattering phase shifts of the DD^* and BB^* systems in the $I = 0$ channel using 2+1 flavor PACS-CS gauge ensembles simulated at $m_\pi = 295$ and 411 MeV. The twisted boundary condition allows us to treat any small momentum on the lattice through the variation of the twist angle, continuously. Therefore, we can determine the low-energy scattering phase shifts near the threshold, where a rapid increase in scattering phase occurs as a precursor to bound state formation. In our simulated pion mass region, we only observed an attractive interaction between D and D^* states in the $I = 0$ channel, which was not strong enough to form bound states. However, for the case of BB^* , we observe that the unitary limit is reached at $m_\pi = 295$ MeV, and the peculiar behavior of the scattering phase shift appears at $E = 0$ MeV. This suggests the formation of a shallow bound state. We can therefore expect a deeply bound state at lighter pion masses at least for the BB^* system.

Acknowledgments

M. N. is supported by Graduate Program on Physics for the Universe (GP-PU) of Tohoku University. Numerical calculations in this work were partially performed using Yukawa-21 at the Yukawa Institute Computer Facility. This work was also supported in part by Grant-in-Aids for Scientific Research from the Ministry of Education, Culture, Sports, Science and Technology (No. 22K03612) and JSPS Research Fellows (No. 24KJ0412).

References

- [1] R. Aaij *et al.* [LHCb], *Nature Phys.* **18**, no.7, 751-754 (2022).
- [2] R. Aaij *et al.* [LHCb], *Nature Commun.* **13**, no.1, 3351 (2022).
- [3] A. V. Manohar and M. B. Wise, *Nucl. Phys. B* **399**, 17-33 (1993).
- [4] L. R. Dai, E. Oset, A. Feijoo, R. Molina, L. Roca, A. M. Torres and K. P. Khemchandani, *Phys. Rev. D* **105**, no.7, 074017 (2022) [erratum: *Phys. Rev. D* **106**, no.9, 099904 (2022)].
- [5] M. Lüscher, *Nucl. Phys. B* **354**, 531-578 (1991).
- [6] S. Ozaki and S. Sasaki, *Phys. Rev. D* **87**, no.1, 014506 (2013).
- [7] M. Padmanath and S. Prelovsek, *Phys. Rev. Lett.* **129**, no.3, 032002 (2022).
- [8] S. Collins, A. Nefediev, M. Padmanath and S. Prelovsek, *Phys. Rev. D* **109**, no.9, 094509 (2024).
- [9] S. Chen, C. Shi, Y. Chen, M. Gong, Z. Liu, W. Sun and R. Zhang, *Phys. Lett. B* **833**, 137391 (2022).
- [10] Y. Lyu, S. Aoki, T. Doi, T. Hatsuda, Y. Ikeda and J. Meng, *Phys. Rev. Lett.* **131**, no.16, 161901 (2023).
- [11] M. L. Du, A. Filin, V. Baru, X. K. Dong, E. Epelbaum, F. K. Guo, C. Hanhart, A. Nefediev, J. Nieves and Q. Wang, *Phys. Rev. Lett.* **131**, no.13, 131903 (2023).
- [12] S. Sasaki and T. Yamazaki, *Phys. Rev. D* **74**, 114507 (2006).
- [13] S. Aoki *et al.* [PACS-CS Collaboration], *Phys. Rev. D* **79**, 034503 (2009).
- [14] S. Aoki, Y. Kuramashi and S. i. Tominaga, *Prog. Theor. Phys.* **109**, 383-413 (2003).
- [15] Y. Kayaba *et al.* [CP-PACS], *JHEP* **02**, 019 (2007).
- [16] T. Kawanai and S. Sasaki, *Phys. Rev. D* **85**, 091503 (2012).